Journal of Solid State Chemistry 185 (2012) 160–165

Contents lists available at SciVerse ScienceDirect

Journal of Solid State Chemistry

journal homepage: www.elsevier.com/locate/jssc

Investigation of the iron site localization in doped ZnO

M.D. Carvalho [a,*], L.P. Ferreira [b], R.P. Borges [c], M. Godinho [c]

[a] CCMM/Dep. Química e Bioquímica, FCUL, 1749-016 Lisboa, Portugal
[b] CFMC, FCUL, 1749-016 Lisboa, Dep. Física, FCTUC, 3004-516 Coimbra, Portugal
[c] CFMC/Dep. Física, FCUL, 1749-016 Lisboa, Portugal

ARTICLE INFO

Article history:
Received 6 August 2011
Received in revised form
14 October 2011
Accepted 3 November 2011
Available online 12 November 2011

Keywords:
Iron doped zinc oxide
Mössbauer spectroscopy
Magnetic semiconductor

ABSTRACT

Iron doped (5%) ZnO powders were prepared by hydrothermal and combustion methods. Subsequent heating treatments on these samples were performed under air and also under a reductive atmosphere. Powder XRD, Mössbauer spectroscopy and magnetization studies were used to characterize the products and investigate the localization of iron ions in the ZnO lattice. It was shown that a mixture with a $ZnFe_2O_4$ type phase was obtained when the sample was prepared by the hydrothermal method, while Fe^{3+} occupy tetrahedral sites of the ZnO lattice in the case of the sample obtained by the combustion method. The magnetic measurements show that no ferromagnetism was detected in the iron doped ZnO compound, neither in the as prepared state nor after reduction.

1. Introduction

ZnO has been one of the most investigated oxides in recent years, especially due to its applications in opto-electronic devices [1]. Zno has many industrial applications as an additive in plastics, ceramics, glasses, cement, rubber, pigments, etc. It is also being investigated for use in photocatalysis and UV-absorbers in textiles and for gas sensor applications [2–4].

ZnO presents the hexagonal wurtzite structure, with Zn^{2+} ions occupying tetrahedral coordination sites. The prediction that the partial substitution of Zn by a transition metal ion in the ZnO structure could lead to a ferromagnetic interaction with Curie temperature (T_C) above room temperature [5–7] stimulated the study of this type of compounds in the form of single crystals, films or powders. In spite of a large amount of research work, the disparity as well as the poor reproducibility of the reported results [8,9] has raised doubts about the feasibility of intrinsic diluted magnetic semiconducting behavior at room temperature. This difficulty is related to the low solubility limits of various transition metal ions in ZnO. In thin films [10] and nanocrystalline powders [11] it was shown that the solubility limit for Fe was lower than 5 mol%. Furthermore, doping with transition metals such as iron, for which M^{3+} ions are highly stable, implies a charge neutrality mechanism, namely the creation of cation vacancies, as proved by positron annihilation lifetime spectroscopy measurements [12]. Various studies on iron doped ZnO samples have reported the coexistence of Fe^{2+} and Fe^{3+} in diluted samples showing ferromagnetism at room temperature [13–15]. The observation of Fe^{3+} has been associated with Zn vacancies that in turn should contribute to the ferromagnetic coupling of the Fe ions.

In order to clarify the iron valence and magnetic ordering in these compounds, we have prepared bulk Fe-doped ZnO by two different routes. Iron was chosen as doping transition metal for two reasons. First, Fe-doped ZnO is one of the candidates to show a ferromagnetic behavior. Furthermore, Fe doping allows the study of the compound by Mössbauer spectroscopy, a powerful local probe technique that should lead to unquestionable conclusions about the location of the Fe ions in the ZnO lattice.

2. Experimental section

Both ZnO and 5% Fe-doped ZnO ($Zn_{0.95}Fe_{0.05}O$) were prepared by the hydrothermal method at 150 °C, and by a self-combustion method at 500 °C. ZnO and Fe:ZnO samples obtained by both methods were white and yellowish, respectively.

(a) Hydrothermal method (H)—Stoichiometric amounts of $Zn(Ac)_2 \cdot 2H_2O$ (Riedel-de-Haën; 99.5%) and $Fe(C_2O_4) \cdot 2H_2O$ (Riedel-de-Haën; 99.5%) (for the doped samples) necessary to prepare ~3 g of product were dissolved in nitric acid solution. Then, the amount of a 4 M ammonium solution necessary to ensure total precipitation was added dropwise under vigorous stirring. The resulting suspension was maintained at room temperature overnight and filtered. This precursor was heated at 150 °C for 2 h in an autoclave, with 20 ml of ammonium solution. The final powder was carefully washed with

* Corresponding author. Fax: +351 21 750 00 88.
E-mail address: mdcarvalho@fc.ul.pt (M.D. Carvalho).

0022-4596/$ - see front matter © 2011 Elsevier Inc. All rights reserved.
doi:10.1016/j.jssc.2011.11.006

deionised water until a neutral pH was obtained, and filtered. In order to check out the stability and the possible presence of impurities, these powders were further calcined until 500 °C, also allowing the comparison with the samples obtained by the self-combustion route.

(b) Self-combustion method (C)—Stoichiometric amounts of $Zn(Ac)_2 \cdot 2H_2O$ and $Fe(C_2O_4) \cdot 2H_2O$ necessary to prepare ~3 g of product were dissolved in nitric acid solution. Then the amount of citric acid equal to the molar amount of product was added. The light-yellow solution was gently heated in a sand bath to evaporate the solution and induce the auto-combustion, which occurred without flame. The yellowish product was further calcined in air at 400 °C for 4 h followed by a treatment at 500 °C for 12 h.

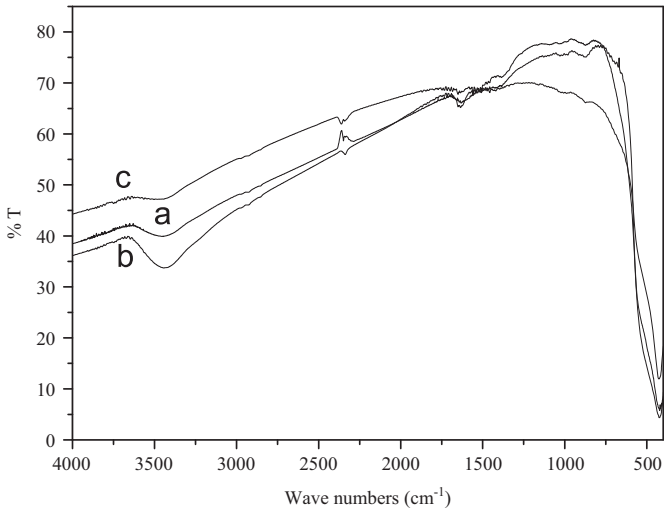

Fig. 1. FTIR spectra of KBr discs of the samples prepared by the self-combustion method: (a) undoped ZnO; (b) Fe:ZnO obtained at 500 °C under air; and (c) Fe:ZnO obtained at 500 °C under hydrogen atmosphere.

In order to investigate the stability of iron (Fe^{3+}/Fe^{2+}) substituting zinc ions in the ZnO lattice, both doped samples were further heated at 500 °C under a reducing atmosphere ($N_2+5\%H_2$) at atmospheric pressure. No color changes were detected after reduction of the iron doped sample obtained by the hydrothermal method while the one prepared by the self-combustion method became green.

The crystal structure and phase purity of the powders were checked by powder X-ray diffraction (XRD) with a Phillips PW 1730 diffractometer using the Cu$K\alpha$ radiation, previously calibrated using a Si standard. Data were collected in the range 20–120° (2θ). The cell parameters were calculated using FullProf [16]. A sixth order polynomial function was used to model the background level and the peak shapes were fitted to a pseudo-Voigt function. Fourier transform infrared spectra (FTIR) of the samples obtained by the self-combustion method were recorded using a Perkin-Elmer 1600 spectrometer at room temperature, as KBr pellets.

The ^{57}Fe Mössbauer spectra were collected at room temperature in transmission mode using a conventional constant-acceleration spectrometer and a 25 mCi ^{57}Co source in an Rh matrix. The velocity scale was calibrated using an α-Fe foil. The spectra were fitted to Lorentzian lines using the WinNormos fitting program.

Magnetization measurements as a function of temperature, $M(T)$, and applied magnetic field, $M(H)$ in doped and undoped ZnO samples, were performed using a SQUID magnetometer (Quantum Design MPMS). The $M(T)$ curves were obtained at 5 mT and 10 mT for temperatures ranging from 2 to 380 K. Data were collected in increasing temperature after both zero-field cooling (ZFC) and field cooling (FC). The isothermal $M(H)$ curves and hysteresis loops were measured for magnetic fields up to 5.5 T.

3. Results and discussion

The FTIR spectra of the samples obtained by the self-combustion method are shown in Fig. 1, where the fundamental vibration

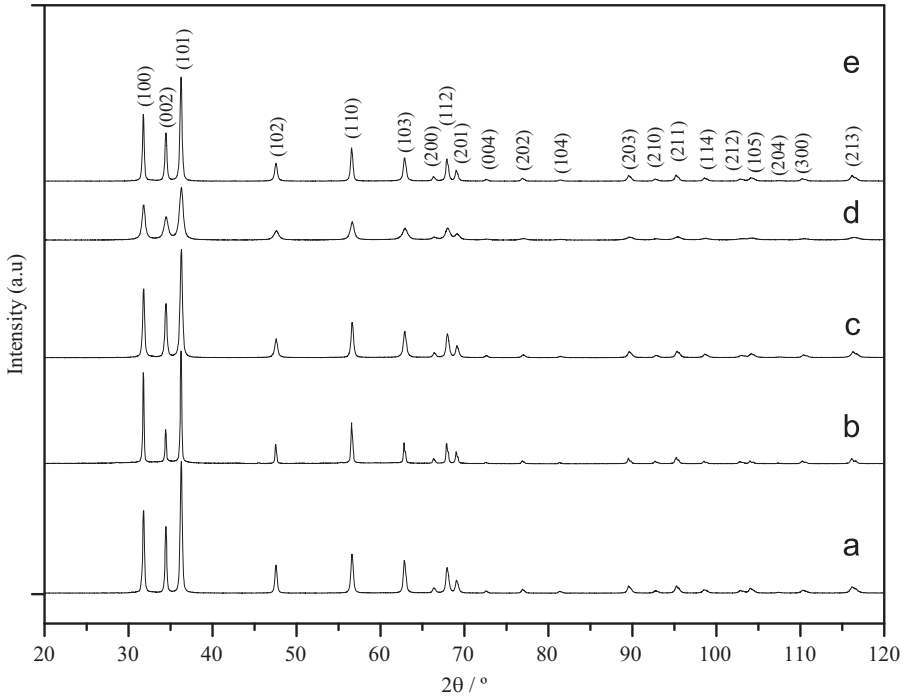

Fig. 2. XRD patterns of the prepared samples obtained by the hydrothermal method (H) and self-combustion route (C): (a) ZnO (H); (b) Fe:ZnO (H); (c) ZnO (C); (d) Fe:ZnO (C); and (e) Fe:ZnO (C) heated under hydrogen atmosphere.

absorption of the zinc oxide is clearly visible at $<520\ cm^{-1}$, and the bands around 3450–3500 cm^{-1} and 1630 cm^{-1} are due to the presence of adsorbed water [3,17]. The lack of other significant absorption bands is indicative of the good degradation of the organic material.

Powder X-ray diffraction (XRD) was used to verify the purity of the synthesized samples and to determine the cell parameters values. The XRD patterns of all as-prepared samples and of the doped sample obtained by the self-combustion method and further reduced under hydrogen atmosphere are presented in Fig. 2. All the patterns indicate the formation of pure ZnO phases, with a hexagonal würtzite structure (space group $P6_3mc$) as no additional diffraction peaks were detected within the X-ray detection limit.

Motivated by the Mössbauer results (see below), the Fe:ZnO sample obtained by the hydrothermal route was further calcined above 200 °C and the peaks of a spinel phase ($ZnFe_2O_4$ type) emerged, being clearly visible after the treatment at 500 °C, as can be observed in Fig. 3. Therefore, it can be deduced that a spinel type phase, with very low crystallinity, was probably present in the as-prepared sample, although not visible by XRD, questioning the effective substitution of zinc by iron ions in the ZnO lattice. This hypothesis is in accordance with the absence of color change in this sample after treatment under reductive atmosphere.

The cell parameter values obtained by the refinement of the XRD patterns using the Fullprof software are summarized in Table 1. The values of the ZnO cell lattice prepared by the self-combustion method are quite identical to those previously reported for a sample obtained by the low-temperature decomposition of acetate solution ($a=3.249$ Å, $c=5.206$ Å) [18], and slightly different from those obtained for the ZnO sample prepared by the hydrothermal route. In the case of the doped compound a slight decrease of the cell parameters when compared to those of the undoped ZnO is observed for the self-combustion samples. The almost insignificant increase verified for the Fe:ZnO sample obtained by the hydrothermal route is consistent with the previous assumption that in this case, iron doping ZnO was not achieved, and iron is certainly present as an impurity phase such as $ZnFe_2O_4$.

Besides, a small increase of the lattice volume was observed when the iron doped sample (self-combustion route) was heated under hydrogen atmosphere. These results are consistent with the effective ionic radius of the several ions involved, considering the fourfold coordination: $Zn^{2+}=0.60$ Å; $Fe^{2+}=0.63$ Å and $Fe^{3+}=0.49$ Å [19]. Thus, it is possible to deduce that the iron probably exists as Fe^{3+} in the Fe:ZnO compound obtained under air and that a reduction of iron occurred when the compound was subject to the hydrogen atmosphere treatment, as effectively demonstrated by the Mössbauer spectroscopy results (see below).

Fig. 2 also indicates that the XRD peaks of the doped sample obtained by the self-combustion method are broadened when

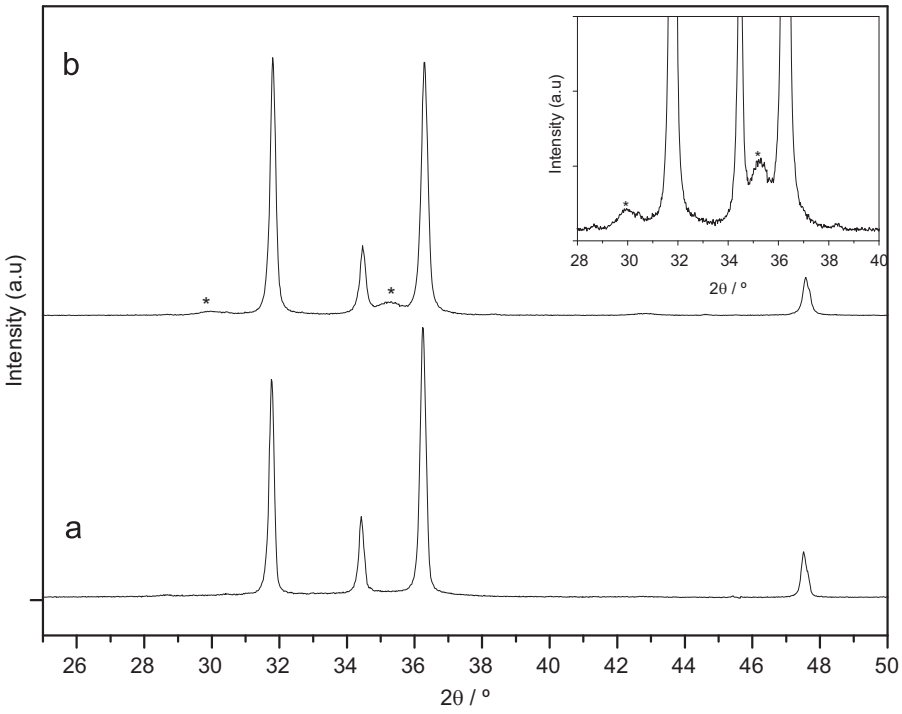

Fig. 3. XRD patterns of the iron doped ZnO samples prepared by the hydrothermal method: (a) as-prepared and (b) after heating at 500 °C, under air. *Diffraction peaks for $ZnFe_2O_4$ shown in detail in the inset.

Table 1
Lattice parameters of the prepared samples.

Preparation method	Sample	a (Å)	c (Å)	Volume (Å^3)
Hydrothermal method	ZnO	3.2518(1)	5.2092(1)	47.702(2)
	Fe:ZnO	3.2523(1)	5.2095(2)	47.721(3)
Self-combustion method	ZnO	3.2498(1)	5.2067(2)	47.620(2)
	Fe:ZnO	3.2493(2)	5.2038(4)	47.580(5)
	Fe:ZnO (reduced)	3.2527(1)	5.2055(2)	47.694(2)

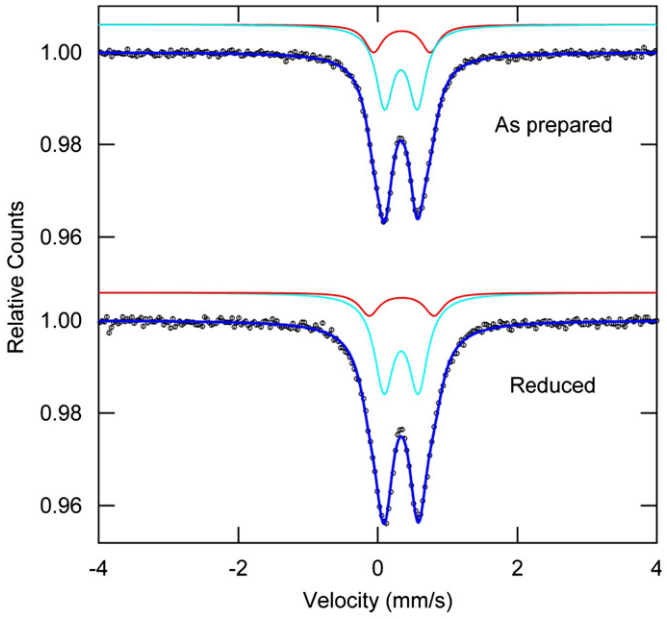

Fig. 4. Mössbauer spectra of the samples prepared by the hydrothermal method.

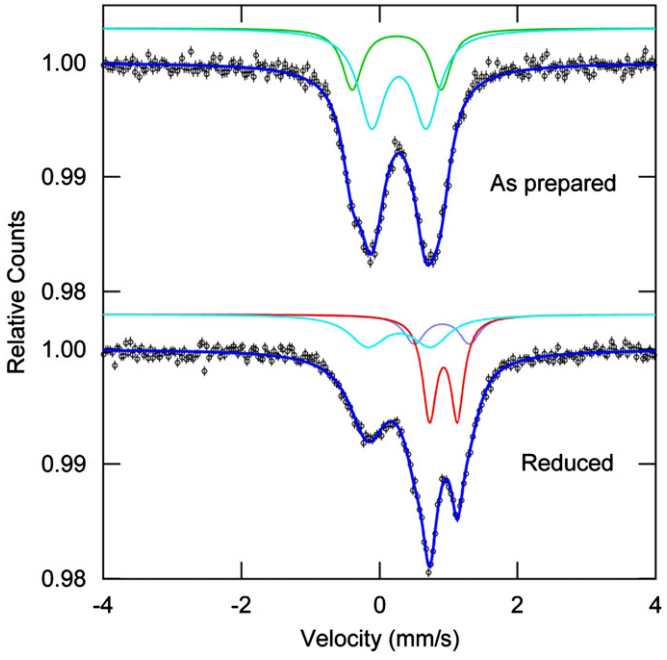

Fig. 5. Mössbauer spectra of the samples prepared by the combustion method.

Table 2
Hyperfine parameters extracted from fitting the Mössbauer spectra for the different compounds. δ: isomer shift; Δ: quadrupole splitting; Γ: line width. Uncertainties in % are less than 2%.

Method	Sample	Site	δ (mm/s)	Δ (mm/s)	Γ (mm/s)	%
Hydrothermal	As prepared	I	0.34(1)	0.44(1)	0.27(1)	55
		II	0.35(1)	0.73(2)	0.34(1)	45
	After reduction	I	0.33(1)	0.42(1)	0.26(2)	42
		II	0.34(1)	0.72(3)	0.43(1)	58
Self-combustion	As prepared	I′	0.28(1)	0.79(2)	0.46(1)	73
		II′	0.24(1)	1.28(2)	0.35(3)	27
	After reduction	I′	0.28(1)	0.91(2)	0.64(2)	54
		II′	0.92(1)	0.41(1)	0.24(2)	28
		III′	0.91(1)	0.82(5)	0.38(5)	18

compared with the XRD patterns of the undoped sample. This feature was previously explained by the possible inhibition of crystallization due to the Fe doping into the ZnO crystal [20].

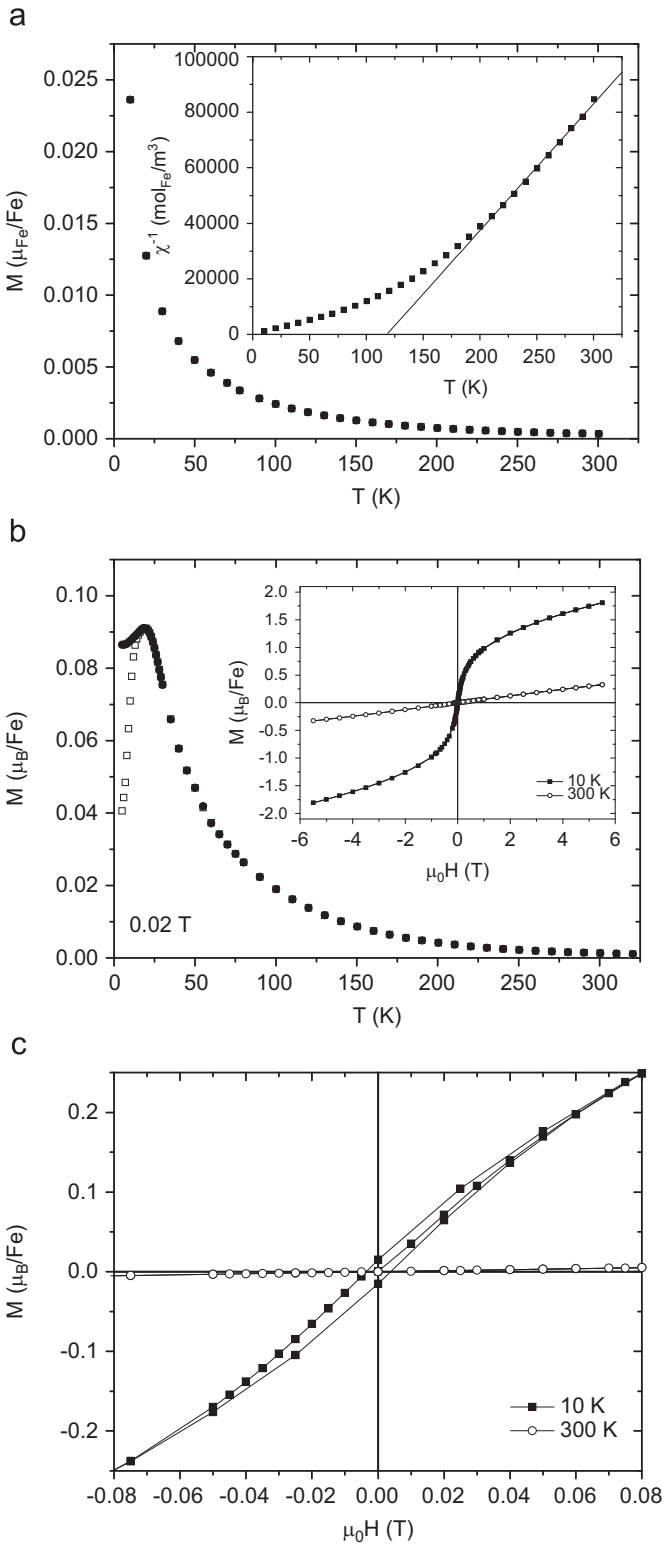

Fig. 6. ZFC (open symbols) and FC (solid symbols) magnetization curves of the samples prepared by the hydrothermal method: (a) as prepared, the inset represents the inverse susceptibility curve; (b) reduced, the inset shows the isothermal magnetization curves at 10 and 300 K; and (c) low field region of the magnetization curves shown in the inset of (b).

The Mössbauer spectra and the results obtained from the fitting procedure for all samples are presented in Figs. 4 and 5 and in Table 2.

Concerning the sample prepared by the hydrothermal route, the spectrum is well resolved using two doublets (Fig. 4) characterized by similar isomer shifts and different quadrupole splittings. The δ values obtained are lower than expected for Fe^{2+} in tetrahedral sites but higher than the usual values for Fe^{3+} in the same kind of sites. In fact, the δ values are much closer to characteristic values of octahedral Fe^{3+} ions ($\delta \approx 0.36$ mm s^{-1}), with one of the ^{57}Fe nucleus sensing a more distorted surrounding (higher quadrupole splitting). These results closely follow the ones obtained by Stewart et al. [21] for $ZnFe_2O_4$ synthesized by a hydrothermal process. Besides, as can be seen in Table 2, no significant differences were found in the hyperfine parameters obtained for the sample measured after the reduction treatment. Therefore, the Mössbauer measurements, together with the magnetization results (see below) and in accordance with XRD data discussion, indicate that iron ions were mainly present in a secondary undesired phase like $ZnFe_2O_4$, stable under reductive atmosphere, justifying the unchanged color of the sample.

Concerning the results obtained for the sample prepared by the self-combustion method, the Mössbauer spectrum is well resolved using two doublets with δ values consistent with the

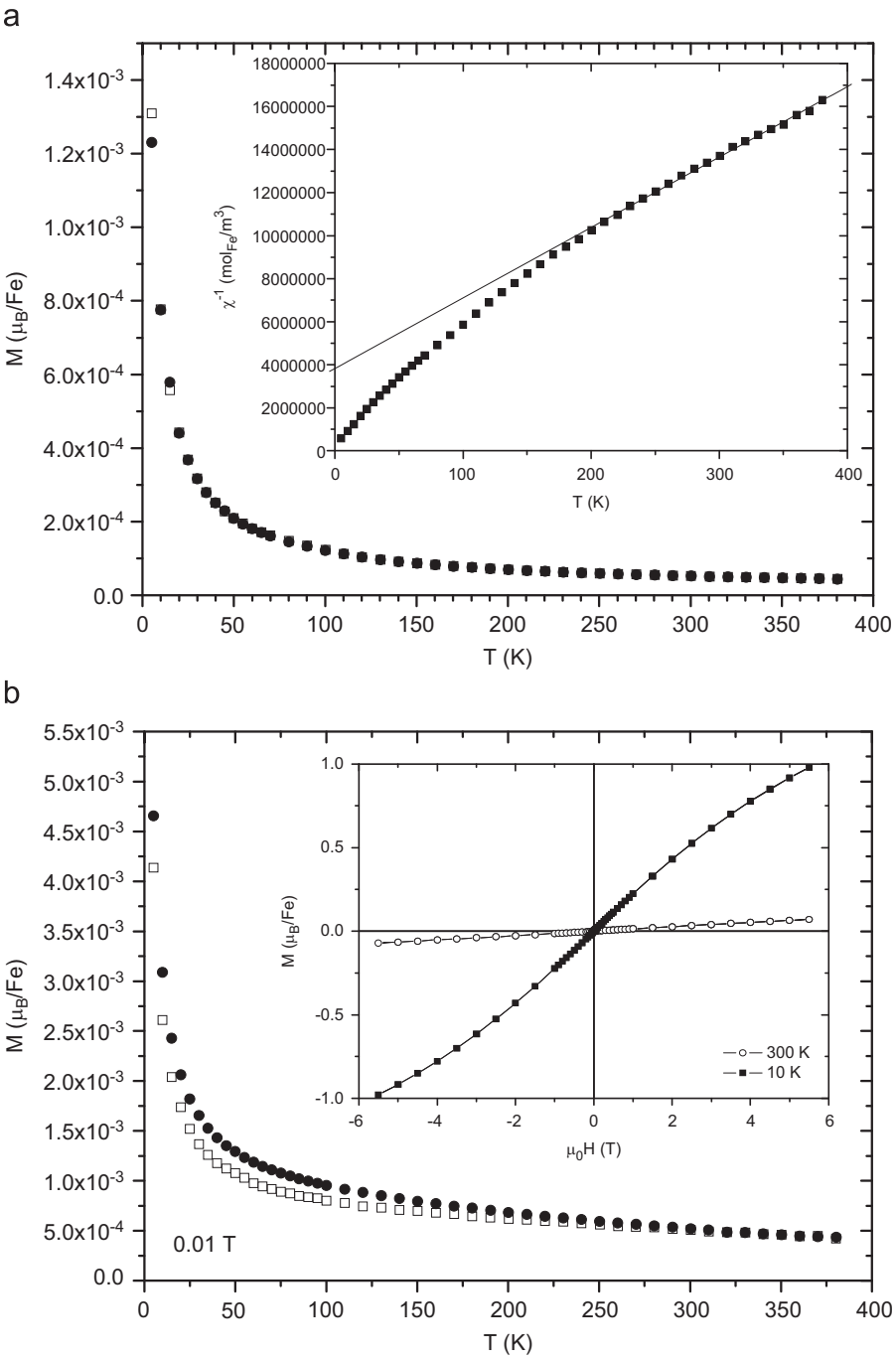

Fig. 7. ZFC (open symbols) and FC (solid symbols) magnetization curves of the samples prepared by the combustion method: (a) as prepared; the inset represents the inverse susceptibility as a function of temperature and the fit to the high temperature data using the Curie–Weiss law and (b) reduced, the inset shows the isothermal magnetization curves obtained at 10 and 300 K.

presence of Fe^{3+} in tetrahedral distorted sites (Fig. 5). According to previous published works, depending on the synthesis conditions, either Fe^{2+} or Fe^{3+} have been detected by Mössbauer spectroscopy substituting Zn^{2+} in the ZnO lattice [22]. In the present work, as Fe^{3+} substituted Zn^{2+}, compensating defects such as cation vacancies had to be formed to maintain charge neutrality. This fact has certainly changed the possible iron vicinities, justifying the spectrum fitting with two distinct Fe^{3+} sites with non-negligible line widths. For this sample, the heating treatment under H_2 reduced Fe^{3+} to Fe^{2+} as undoubtedly shown by the two doublets with δ values around 0.9 mm/s (about 50% of the iron ions). Further reduction treatment did not increase the Fe^{2+} content.

Fig. 6 shows the magnetization curves of the samples obtained by the hydrothermal method. As can be seen, in the case of the as-prepared sample the magnetization decreases with temperature over the whole temperature range. The inverse DC susceptibility curve (inset) shows a linear dependence with temperature at the highest temperatures and from the fitting with the Curie–Weiss law the value of 5.4(1) μ_B for the effective magnetic moment and a positive paramagnetic Curie temperature were extracted. However, as previously shown by XRD (Fig. 3), a $ZnFe_2O_4$ type phase is also present in this sample. After the reduction treatment, which in this case did not change the iron valence, as proved by the Mössbauer results, the existence of a $ZnFe_2O_4$ type phase is clearly identified by the magnetization maximum around 19 K, observed in both ZFC and FC curves. In fact, normal $ZnFe_2O_4$ with all Zn ions in tetrahedral sites and all Fe ions in octahedral sites has a Néel temperature of 10 K, but cation disorder leads to ferromagnetic interactions and an increase of the critical temperature. Isothermal magnetization at 10 K clearly shows a ferromagnetic behavior in agreement with the presence of a $ZnFe_2O_4$ type phase.

The magnetization results of the samples obtained by the combustion method are presented in Fig. 7. For the as-prepared sample, the inverse DC susceptibility curve (inset in Fig. 7a) shows a linear dependence with temperature. A value of 4.4(1) μ_B for the effective magnetic moment and a negative paramagnetic Curie temperature (around -110 K) were extracted using the Curie–Weiss law at the highest temperatures. The moment obtained is lower than the expected value for Fe^{3+} ($p=5.9$). The negative value of θ indicates the existence of antiferromagnetic interactions that could lower the effective magnetic moment. After the reduction treatment (Fig. 7b) the sample still displays a paramagnetic behavior, although an irreversibility can be clearly observed for temperatures up to 300 K. Isothermal magnetization measured at 10 K also shows a paramagnetic behavior. Since no magnetic transition is detected in the entire range of temperatures, the irreversibility behavior may be understood as a consequence of the 50% of Fe^{2+} present in the sample, with an enhancement of the local Fe–Fe interaction. The Mössbauer results of this sample clearly indicated that only the valence of iron ions was changed with the reduction treatment, with iron ions remaining in tetrahedral coordination, supporting the idea of a diluted system. In such type of system a mean field model (RKKY interaction) has been previously invoked to explain the magnetization irreversibility observed in cobalt doped ZnO samples [23] and a similar mechanism is a possible explanation for the present results. Room temperature ferromagnetic order in transition-metal doped ZnO has been reported by other authors and explained through a bound magnetic polaron model [24], where lattice defects play a key role in coupling the magnetic moments of transition-metal ions. The Mössbauer results described in this work suggest the presence of lattice defects but such defects seem to have no role in mediating a magnetic ordered state of the Fe ions. The magnetization results obtained with the samples prepared by the combustion method clearly show that 5% Fe diluted in ZnO does not exhibit a ferromagnetic behavior.

4. Conclusions

In this work, distinct samples were obtained using two different synthesis methods. Although, a single phase was apparently present on the as-prepared sample synthesized by the hydrothermal method, the results obtained by the different techniques are consistent with the formation of a $ZnFe_2O_4$ type phase mixed with ZnO. On the contrary, the compound $Zn_{0.95}Fe_{0.05}O$ was successfully synthesized by a self-combustion method, as it was demonstrated that Fe^{3+} occupy tetrahedral sites of the ZnO lattice. Furthermore, it has been shown that this compound is structurally stable under hydrogen atmosphere, leading to partial reduction of Fe^{3+} to Fe^{2+}, as undoubtedly proved by Mössbauer spectroscopy. This valence change was also evident by a change of color. Globally, the magnetization measurements indicated that both as-prepared and reduced $Zn_{0.95}Fe_{0.05}O$ compounds display a paramagnetic behavior and, contrary to some results published in the literature, no ferromagnetism was detected in these 5% doped ZnO semiconductors.

References

[1] A.B. Djurišić, A.M.C. Ng, X.Y. Chen, Prog. Quantum Electron. 34 (2010) 191–259.
[2] S. Rehman, R. Ullah, A.M. Butt, N.D. Gohar, J. Hazard. Mater. 170 (2009) 560–569.
[3] A. Becheri, M. Dürr, P. Lo Nostro, P. Bagliono, J. Nanopart. Res. 10 (2008) 679–689.
[4] C.S. Rout, A.R. Raju, A. Govindaraj, C.N.R. Rao, Solid State Commun. 138 (2006) 136–138.
[5] T. Dietl, H. Ohno, M. Matsukura, J. Cibert, D. Ferrand, Science 287 (2000) 1019–1022.
[6] K. Sato, H.K. Yoshida, Jpn. J. Appl. Phys. 39 (2000) L555–L558.
[7] K. Sato, H.K. Yoshida, Jpn. J. Appl. Phys. 40 (2001) L334–L336.
[8] G.V. Lashkarev, M.V. Radchenko, V. Karpina, V. Sichkovskyi, Low Temp. Phys. 33 (2007) 165–173.
[9] S.B. Ogale, Adv. Mater. 22 (2010) 3125–3155.
[10] Z. Jin, T. Fukumura, M. Kawasaki, K. Ando, H. Saito, T. Sekiguchi, Y.Z. Yoo, M. Murakami, Y. Matsumoto, T. Hasegawa, H. Koinuma, Appl. Phys. Lett. 78 (2001) 3824.
[11] S.K. Mandal, A.K. Das, T.K. Nath, D. Karmakar, Appl. Phys. Lett. 89 (2006) 144105.
[12] A.K. Mishra, D. Das, Mater. Sci. Eng. B 171 (2010) 5–10.
[13] D. Karmakar, S.K. Mandal, R.M. Kadam, A.K. Rajarajan, T.K. Nath, A.K. Das, I. Dasgupta, G.P. Das, Phys. Rev. B. 75 (2007) 14404.
[14] H. Liu, J. Yang, Y. Zhang, Y. Wang, M. Wei, Mater. Chem. Phys. 112 (2008) 1021–1023.
[15] M.V. Limaye, S.B. Singh, R. Das, P. Poddar, S.K. Kulkarni, J. Solid. State Chem. 184 (2011) 391–400.
[16] T. Roisnel, J. Rodriguez-Carvajal, FullProf Suite (2005).
[17] S. Maensiri, P. Laokul, V. Promarak, J. Cryst. Growth 289 (2006) 102–106.
[18] C.N.R. Rao, F.L. Deepak, J. Mater. Chem. 15 (2005) 573–578.
[19] R.D. Shannon, Acta Cryst., A. 32 (1976) 751–767.
[20] H. Liu, J. Yang, Y. Zhang, L. Yang, M. Wei, X. Ding, J. Phys. Condens Matter 21 (2009) 145803.
[21] S.J. Stewart, S.J.A. Figueroa, M.B. Sturla, R.B. Scorzelli, F. García, F.G. Requejo, Physica B 389 (2007) 155–158.
[22] R. Wang, A.W. Sleight, M.A. Subramanian, J. Solid State Chem. 125 (1996) 224–227.
[23] B. Martíez, F. Sandiumenge, Ll. Balcells, J. Arbiol, F. Sibieude, C. Monty, Phys. Rev. B. 72 (2005) 165202.
[24] J.M.D. Coey, A.P. Douvalis, C.B. Fitzgerald, M. Venkatesan, Appl. Phys. Lett. 84 (2004) 1332–1334.